

ACTIVE BEAM TRACKING WITH RECONFIGURABLE INTELLIGENT SURFACE

Han Han, Tao Jiang and Wei Yu

Electrical and Computer Engineering Department
University of Toronto, Canada

ABSTRACT

This paper studies a beam tracking problem in a reconfigurable intelligent surface (RIS)-assisted communication system, in which a single antenna access point (AP) tracks a single-antenna mobile user equipment (UE) through actively reconfiguring the RIS. To maintain beam alignment over time, the mobile UE periodically sends a sequence of pilots to the AP in the uplink, and the AP updates the RIS reflection coefficients for both the subsequent downlink data transmission and uplink pilot reception stages in a sequential fashion. This is an *active sensing* problem which is analytically intractable. This paper proposes a deep learning framework to solve this problem. We use a neural network architecture based on long short-term memory (LSTM) in which the LSTM cell automatically summarizes the time-varying channel information based on periodically received pilots into a state vector, and the state vector is mapped to the RIS reflection coefficients for subsequent downlink data transmission and uplink pilot reception using two additional deep neural networks (DNNs). Simulation results show that this proposed active sensing approach is able to maintain beam alignment much more efficiently than traditional data-driven methods based only on channel statistics.

1. INTRODUCTION

Reconfigurable intelligent surface (RIS) is a promising technology for integrated sensing and communications due to its ability to reflect incoming signals toward desired directions [1, 2, 3]. The RIS can enhance communication by establishing focused beams between the access point (AP) and the user equipment (UE), but this focusing capability depends crucially on channel sensing. In time-division duplex (TDD) systems with channel reciprocity, channel state information (CSI) acquisition for RIS-assisted systems can be done using uplink pilots [4, 5]. However, in high-mobility scenarios where CSI needs to be obtained more frequently, the existing schemes can lead to significant pilot overhead since they estimate CSI from scratch in each channel sensing phase without exploiting the temporal channel correlation due to UE mobility.

This paper considers the incorporation of *active sensing* [6] for beam tracking in an RIS-assisted mobile communication system, in which a UE periodically sends pilots to the AP through the reflection of an RIS, and the AP designs the downlink RIS reflection coefficients based on the received pilots so that the RIS can maintain beam alignment with the mobile UE over time. Such a beam tracking problem is quite challenging, because both uplink sensing and downlink reflection coefficients need to be designed based on a limited number of pilots over time. This paper proposes an active sensing framework to solve this problem. Specifically, the proposed learning-based approach aims to abstract the temporal correlation of the time-varying channels into a state vector, which can be utilized to design the RIS reflection coefficients for both data transmission and uplink pilot reception in subsequent stages.

The beam/channel tracking problem in RIS-assisted communication systems has been investigated in [7, 8, 9, 10, 11] using techniques such as extended Kalman filter and recurrent neural network (RNN). However, [7, 8, 9] use fixed RIS reflection coefficients generated either randomly or based on the discrete Fourier transform (DFT) [12] during the pilot transmission phases. Such a non-adaptive RIS sensing scheme is far from optimal. Further, these works fall into the paradigm of estimating CSI first, then designing the RIS reflection coefficients, which can be quite suboptimal as compared to directly mapping the received pilots to the optimized RIS reflection coefficients [5, 6, 13, 14]. On the other hand, [10, 11] adaptively design the RIS sensing vector based on an RNN network, but they require the UE positions as the input. In addition, [10, 11] propose to employ the same RIS reflection coefficients in both sensing and data transmission stages. This can be suboptimal due to different functionalities of the RIS in two stages.

This paper proposes to design the RIS sensing vectors and reflection coefficients for uplink pilot reception and downlink beam alignment in an active fashion. Specifically, in the CSI acquisition stages, the RIS sensing vectors are designed based on the pilots received previously. After collecting the next round of pilots, the downlink RIS reflection coefficients for the subsequent data transmission are designed based on all historical observations. This problem of optimally designing the sequential RIS sensing and downlink alignment strategy is challenging, because it requires learning the channel correlations from periodically received pilots and exploring a high-dimensional and nonconvex optimization landscape. To this end, this paper proposes to employ an RNN to automatically summarize the temporal correlations of the time-varying channel into fixed-size state information. Specifically, we choose the long short-term memory (LSTM) variant of the RNN [15] due to its robustness against vanishing and exploding gradients [16], and use its fixed-size cell state to summarize the current channel information. Deep neural networks (DNNs) are then employed to map the LSTM cell state to the optimized RIS coefficients for subsequent sensing and data transmission. Such a learning-based integrated active sensing and communication paradigm can significantly outperform existing non-adaptive beam tracking methods.

2. SYSTEM MODEL AND PROBLEM FORMULATION

2.1. System Model

Consider an RIS-assisted SISO system where a single antenna AP seeks to communicate with a single-antenna mobile UE. As shown in Fig. 1, the RIS with N_r passive elements is placed between the AP and the UE to enable a reflection link, and it works cooperatively with the AP to control the phase of the reflected signals by tuning the phase shifts of each passive element through an RIS controller.

This paper assumes that the RIS-assisted system operates in

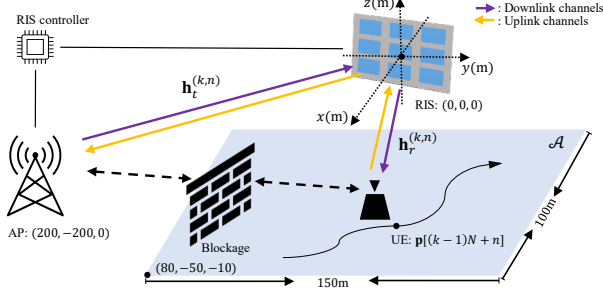


Fig. 1. RIS assisted mobile communication system. In the n th block of the k th transmission frame, $\mathbf{h}_t^{(k,n)}$ and $\mathbf{h}_r^{(k,n)}$ denote the channel between AP and RIS, and between RIS and UE, respectively.

TDD mode with uplink-downlink channel reciprocity, so instantaneous CSI can be obtained based on the uplink pilots. The time-varying channels are split into sufficiently small fixed-length blocks so that the channels within each block can be assumed to remain constant, but the channels are correlated across the blocks. In the 0th block of each frame, the UE sends pilots to the AP so that the AP can update the RIS reflection coefficients to maintain beam alignment in the subsequent N data transmission blocks as shown in Fig. 2.

More precisely, in the pilot stage of the k th transmission frame, UE transmits L pilots $\{x_l^{(k)}\}_{l=1}^L$ to the AP. Without loss of generality, we set $x_l^{(k)} = \sqrt{P_u}$, where P_u is the uplink transmit power. The RIS reflection coefficients for the l th uplink pilot transmission in the k th frame are denoted as $\mathbf{v}_l^{(k)} = [e^{j\theta_1}, e^{j\theta_2}, \dots, e^{j\theta_{N_r}}]^\top \in \mathbb{C}^{N_r}$, where $\theta_i \in [0, 2\pi)$ is the phase shift of the i th passive RIS element. We also refer to the RIS reflection coefficients in the CSI acquisition stages as the sensing vector.

We use $\mathbf{h}_t^{(k,n)} \in \mathbb{C}^{N_r}$ and $\mathbf{h}_r^{(k,n)} \in \mathbb{C}^{N_r}$ to denote the channel between AP and RIS, and between RIS and UE, respectively, in the n th block of the k th frame. For example, in the pilot stage, which corresponds to the 0th block of each frame, the l th pilot received by the AP in the pilot stage of the k th frame is given as:

$$\hat{y}_l^{(k)} = \sqrt{P_u} (\mathbf{h}_t^{(k,0)})^\top \text{diag}(\mathbf{v}_l^{(k)}) \mathbf{h}_r^{(k,0)} + \hat{z}_l^{(k)}, \quad (1a)$$

$$= \sqrt{P_u} (\mathbf{v}_l^{(k)})^\top \mathbf{h}_c^{(k,0)} + \hat{z}_l^{(k)}, \quad (1b)$$

where $\mathbf{h}_c^{(k,0)} \triangleq \text{diag}(\mathbf{h}_t^{(k,0)}) \mathbf{h}_r^{(k,0)} \in \mathbb{C}^{N_r}$ is the cascaded channel between AP and UE in the pilot block of the k th frame, and $\hat{z}_l^{(k)} \sim \mathcal{CN}(0, \sigma_u^2)$ is the additive white Gaussian noise (AWGN) at AP.

2.2. Active Sensing for Beam Tracking with RIS

To minimize the pilot overhead for the RIS-assisted mobile beam tracking, it is crucial that the AP employs an active sensing strategy for designing the RIS sensing coefficients in the pilot phase as well as accounting for the temporal correlations of the time-varying channel (due to UE mobility) in designing the downlink RIS reflection coefficients. Most prior works on RIS-based beam/channel tracking (e.g. [7, 8, 9] and references therein) only exploit the channel correlation information to design the RIS reflection coefficients for the downlink data transmission, while using fixed or random RIS sensing vectors $\{\mathbf{v}_l\}_{l=1}^L$ over the L pilot transmissions. Such a non-adaptive design for the RIS sensing vectors is far from optimal, especially in the scenarios with limited pilot training overhead.

This paper proposes an active sensing based approach in which the RIS reflection coefficients for both pilot and data transmissions

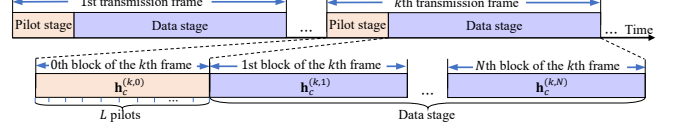


Fig. 2. Frame structure of the proposed transmission protocol.

can be adaptively designed. Specifically, in the pilot stage of the k th transmission frame, the RIS sensing vectors are designed based on the pilots received and the RIS sensing vectors prior to the k th frame as follows:

$$\{\mathbf{v}_l^{(k)}\}_{l=1}^L = \mathcal{G}^{(k)} \left(\left\{ \{\hat{y}_l^{(j)}\}_{l=1}^L \right\}_{j=1}^{k-1}, \left\{ \{\mathbf{v}_l^{(j)}\}_{l=1}^L \right\}_{j=1}^{k-1} \right), \quad (2)$$

where $\mathcal{G}^{(k)} : \mathbb{C}^{L(k-1)} \times \mathbb{C}^{N_r L(k-1)} \rightarrow \mathbb{C}^{N_r L}$ is the active sensing scheme adopted by the RIS controller in the k th frame, and the element of each output vector $\mathbf{v}_l^{(k)}$ should satisfy the unit modulus constraint. After collecting the observations in the pilot stage of the k th frame, we can then design the downlink RIS reflection coefficients $\mathbf{w}^{(k)} \in \mathbb{C}^{N_r}$ for all N blocks in the subsequent data transmission stage of the k th frame based on all historical observations, i.e.,

$$\mathbf{w}^{(k)} = \mathcal{F}^{(k)} \left(\left\{ \{\hat{y}_l^{(j)}\}_{l=1}^L \right\}_{j=1}^k, \left\{ \{\mathbf{v}_l^{(j)}\}_{l=1}^L \right\}_{j=1}^k \right), \quad (3)$$

where $\mathcal{F}^{(k)} : \mathbb{C}^L \times \mathbb{C}^{N_r L k} \rightarrow \mathbb{C}^{N_r}$ is the downlink alignment scheme adopted by the RIS controller in the k th frame, and the element of $\mathbf{w}^{(k)}$ should satisfy the unit modulus constraint.

2.3. Mobile Beam Alignment for Downlink Rate Maximization

The data symbol received at the UE in the n th block of the k th transmission frame can be expressed as:

$$y^{(k,n)} = \sqrt{P_d} (\mathbf{h}_c^{(k,n)})^\top \mathbf{w}^{(k)} s^{(k,n)} + z^{(k,n)}, \quad n=1, \dots, N, \quad (4)$$

where $s^{(k,n)} \in \mathbb{C}$ is the normalized data symbol with $\mathbb{E}[|s^{(k,n)}|^2] = 1$, P_d is the downlink transmit power, $z^{(k,n)} \sim \mathcal{CN}(0, \sigma_d^2)$ denotes the i.i.d. AWGN at UE. Therefore, the downlink data rate in the n th block of the k th transmission frame can be expressed as:

$$R(\mathbf{h}_c^{(k,n)}, \mathbf{w}^{(k)}) = \log_2 \left(1 + \frac{P_d |(\mathbf{h}_c^{(k,n)})^\top \mathbf{w}^{(k)}|^2}{\sigma_d^2} \right). \quad (5)$$

We now state the beam tracking problem for downlink rate maximization as that of designing both the active sensing scheme $\mathcal{G}^{(k)}$ and the downlink alignment scheme $\mathcal{F}^{(k)}$ to maximize:

$$\begin{aligned} & \underset{\mathcal{G}^{(k)}(\cdot, \cdot), \mathcal{F}^{(k)}(\cdot, \cdot)}{\text{maximize}} && \mathbb{E} \left[\sum_{n=1}^N R(\mathbf{h}_c^{(k,n)}, \mathbf{w}^{(k)}) \right] \\ & \text{subject to} && (2), (3). \end{aligned} \quad (6)$$

Here, the expectation is over the channel fading and the uplink noise. Analytically solving this variational optimization problem (6) is challenging, due to the expanding size of the historical data and the high-dimensional function mappings. Specifically, since the evolution of the mobile channel state is a nonlinear function with respect to the measurements, summarizing the historical observations to some fixed-size sufficient statistics, e.g., posterior distribution of the channel parameters, is computationally demanding. Moreover, problem (6) involves a joint optimization over the high-dimensional mappings $\mathcal{G}^{(k)}$ and $\mathcal{F}^{(k)}$, which is highly nontrivial due to the significant computational complexity of exploring the high-dimensional and nonconvex optimization landscape.

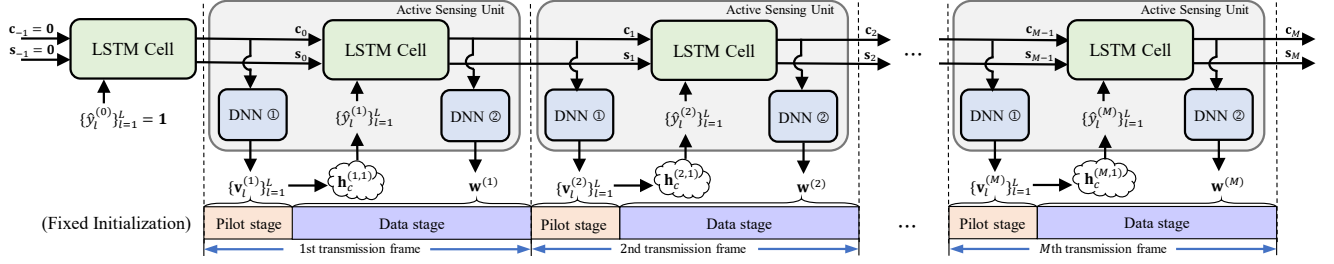


Fig. 3. End-to-end training architecture for the active sensing unit. The concatenated M units correspond to M transmission frames.

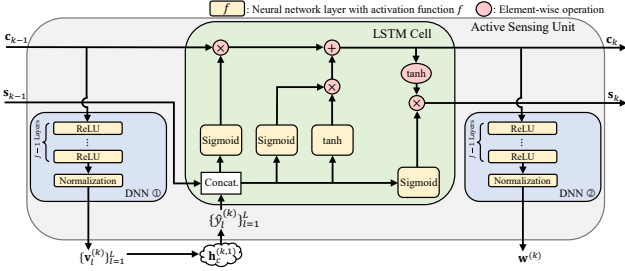


Fig. 4. Active sensing unit for mobile beam alignment with RIS. We set the unit modulus normalization activation function [6] for the final layers of the two DNNs.

3. DATA-DRIVEN APPROACH FOR TRACKING

This paper proposes to employ an end-to-end neural network to directly learn an optimized active sensing strategy from the training data. In this way, the computational complexity of the optimization is transferred to the neural network training process [14]. Specifically, we use an LSTM-based RNN to capture the temporal correlations of the time-varying channel by automatically summarizing the channel variations into a state information vector, which is further processed using DNNs to design the RIS reflection coefficients.

As shown in Fig. 4, the main functionalities of the proposed active sensing unit are as follows: (i) a DNN mapping the previous state vector to the design of the RIS sensing vectors, which are used to collect the pilots sent from the UE at the current pilot stage; (ii) an LSTM cell summarizing the temporal correlations of the time-varying channel by updating the state vector based on the latest received pilots; (iii) another DNN computing the optimized downlink RIS reflection coefficients based on the updated state vector. We use two standalone DNNs to design the reflection coefficients, because it would be too demanding to request an LSTM cell to learn the state vectors and the reflection coefficients simultaneously.

To train such an active sensing unit, we propose to concatenate M active sensing units with tied weights to form a deep neural network as shown in Fig. 3, with each unit corresponding to a transmission frame. By training the concatenated neural network, the active sensing unit is able to explore the temporal channel correlation from the input pilot sequence. The proposed end-to-end architecture is trained in an unsupervised fashion based on the objective (6) averaged over M frames, i.e., $-\frac{1}{M} \sum_{m=1}^M \mathbb{E}[\sum_{n=1}^N R(\mathbf{h}_c^{(m,n)}, \mathbf{w}^{(m)})]$, where the expectation is approximated by the empirical average over the training set. In practice, we choose M to be sufficiently large so that the temporal correlations of the time-varying channel can be learned through the periodically received pilots.

4. NUMERICAL RESULTS AND INTERPRETATIONS

4.1. Simulation Setup

In the Cartesian coordinate system shown in Fig. 1, the AP and a rectangular RIS with $N_r = 64$ passive elements are located at $(200, -200, 0)$ and $(0, 0, 0)$, respectively. In the n th block of the k th transmission frame, we denote the coordinate of the mobile UE as $\mathbf{p}[(k-1)N+n] = (x[(k-1)N+n], y[(k-1)N+n], -10)$.

We use a Markov process to model the mobility of the UE. In the i th time block, the position of the mobile UE is determined by $\mathbf{p}[i] = \mathbf{p}[i-1] + \lambda \Delta \mathbf{d}[i-1]$, where $\Delta \mathbf{d}[i-1] \in \{(-1, 0, 0), (1, 0, 0), (0, -1, 0), (0, 1, 0)\}$ is the direction change of the UE in the $(i-1)$ th block, and λ denotes the distance the UE moves in each block. We assume that $\lambda = 0.043\text{m}$ with probability 90%, and $\lambda = 0.06\text{m}$ with probability 10%. The initial location $\mathbf{p}[1]$ is randomly chosen in a $150\text{m} \times 100\text{m}$ rectangular region \mathcal{A} as shown in Fig. 1, and $\Delta \mathbf{d}[1]$ is chosen from four direction vectors with equal probabilities 25%. To model the typical scenario where the mobile UE mostly moves in one direction, we assume $\Delta \mathbf{d}[i] = \Delta \mathbf{d}[i-1]$ with probability 99.5%, $\Delta \mathbf{d}[i] = -\Delta \mathbf{d}[i-1]$ with probability 0.1%, and $\Delta \mathbf{d}[i]$ to be the other two directions with equal probabilities 0.2%.

In the n th block of the k th transmission frame, the channels from and to the RIS are modeled by the Rician fading as:

$$\begin{cases} \mathbf{h}_t^{(k,n)} = \beta_t \left(\sqrt{\frac{\varepsilon}{1+\varepsilon}} \mathbf{a}_t(\varphi) + \sqrt{\frac{1}{1+\varepsilon}} \tilde{\mathbf{h}}_t^{(k,n)} \right), \\ \mathbf{h}_r^{(k,n)} = \beta_r^{(k,n)} \left(\sqrt{\frac{\varepsilon}{1+\varepsilon}} \mathbf{a}_r(\mathbf{p}[(k-1)N+n]) + \sqrt{\frac{1}{1+\varepsilon}} \tilde{\mathbf{h}}_r^{(k,n)} \right), \end{cases}$$

where \mathbf{a}_t and \mathbf{a}_r are the steering vectors, φ is the angular parameter, and ε is the Rician factor which is set to be 10. The path loss of the AP-IRS link β_t and the IRS-UE link $\beta_r^{(k,n)}$ are modeled as $30 + 22 \log(l_t)$ and $30 + 22 \log(l_r^{(k,n)})$, respectively, where l_t and $l_r^{(k,n)}$ are the distance of the corresponding link [17, Table B.1.2.1-1]. The non-line-of-sight components of the channels are modeled by the stationary Gauss-Markov process as follows [18]:

$$\begin{cases} \tilde{\mathbf{h}}_q^{(k,n)} = \rho_q \tilde{\mathbf{h}}_q^{(k,n-1)} + \sqrt{1 - \rho_q^2} \mu_q^{(k,n-1)}, 2 \leq n \leq N, \\ \tilde{\mathbf{h}}_q^{(k,n)} = \rho_q \tilde{\mathbf{h}}_q^{(k-1,N)} + \sqrt{1 - \rho_q^2} \mu_q^{(k-1,N)}, n = 1, \end{cases} \quad (7)$$

where $q \in \{t, r\}$, correlation coefficient $\rho_t = 0.995$, $\rho_r = 0.99$, perturbation term $\mu_q^{(k,n)} \sim \mathcal{CN}(0, 1)$, and $\tilde{\mathbf{h}}_q^{(1,1)} \sim \mathcal{CN}(0, \mathbf{I})$.

We assume that each transmission frame contains $N = 30$ blocks, and the UE transmits $L = 10$ pilots in each pilot stage. The uplink and downlink transmission power are set to be 15dBm, and

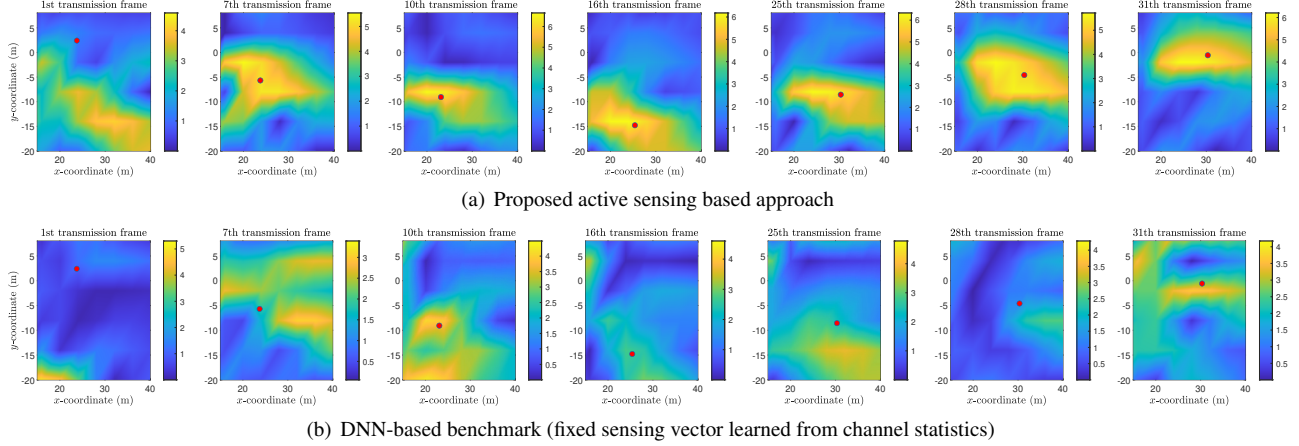


Fig. 5. Instantaneous downlink rate around the position of the mobile UE obtained by methods (a) and (b) in different transmission frames.

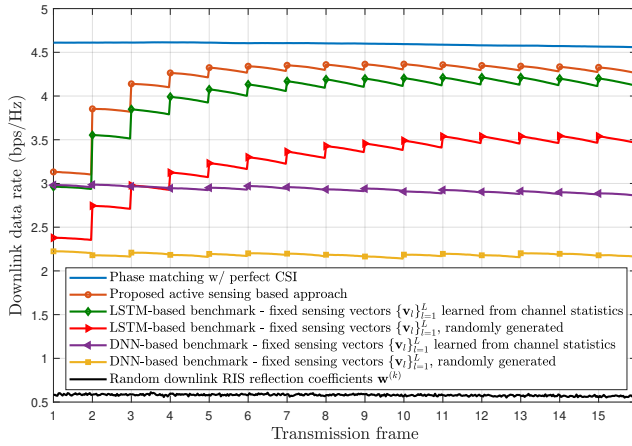


Fig. 6. Downlink rate versus transmission frames for different beam tracking methods with RIS. Each frame contains $N = 30$ blocks.

the noise power of the uplink and the downlink are -105dBm and -115dBm , respectively. We concatenate $M = 10$ active sensing unit in the training phase. The proposed deep learning framework is implemented on TensorFlow [19] using the Adam optimizer [20].

We compare the proposed active sensing based approach with the following benchmarks: (i) given the perfect CSI, calculating the optimal downlink RIS reflection coefficients by matching the phase of \mathbf{h}_c ; (ii) employing a similar LSTM network as the proposed approach, but with fixed RIS sensing vectors $\{\mathbf{v}_l\}_{l=1}^L$ for all pilot stages; (iii) at each frame, employing a fully connected DNN to map the L received pilots to the downlink RIS reflection coefficients with fixed sensing vectors; (iv) randomly generating the phase of $\mathbf{w}^{(k)}$ for each data stage. In both (ii) and (iii), the phase of each fixed sensing vector is generated either randomly or learned from statistics of the training data [6].

4.2. Numerical Results and Visual Interpretations

Fig. 6 shows the downlink data rates obtained by different mobile beam tracking methods in each transmission frame. Each value is averaged over 3000 randomly generated UE moving trajectories. The

peaks on the lines indicate that the rates are prevented from losing too much due to the update of the downlink RIS reflection coefficients based on the latest received pilots, which contain the latest information on the time-varying channels. Within each frame, the data rate slightly decreases by about 2% due to reusing the downlink RIS reflection coefficients for 30 blocks, while the channels slowly change over time. Under fixed sensing schemes, the benchmarks with the learned sensing vectors outperform those with random sensing vectors, since the RIS coefficients are learned based on the distributions of the training set. With learned sensing vectors, the LSTM-based benchmark outperforms the DNN-based benchmark for downlink RIS coefficient design, since the LSTM-based method is able to leverage the temporal channel correlations. Moreover, the proposed active sensing based approach performs better than the benchmarks with learned sensing vectors, because the active sensing approach further uses implicit trajectory information to adaptively update the RIS sensing vectors. In conclusion, the best performance is achieved when *both* the RIS sensing vectors and downlink reflection coefficients are adaptively designed.

In Fig. 5, we plot the instantaneous downlink rate map around the location of the mobile UE (red dots in Fig. 5) in the first block of each frame to illustrate that the proposed approach designs interpretable downlink RIS reflection coefficients. By exploiting channel correlations to update both the RIS sensing and downlink reflection coefficients, the proposed approach indeed keeps track of the UE by successively aligning the downlink RIS reflected beam towards the location of the UE, thus maximizing the rate. The DNN-based benchmark, which learns fixed sensing vectors from statistics of the training data, performs poorly because it needs more pilots to design the RIS reflection coefficients for data transmission in each frame.

5. CONCLUSION

This paper proposes an active sensing based mobile beam tracking approach for the RIS-assisted system. By employing a LSTM-based deep learning framework, the proposed approach can adaptively update *both* RIS sensing vectors and downlink reflection coefficients in each transmission frame based on the received pilots. Numerical results show that under the same pilot overhead, the proposed active sensing based approach indeed generates interpretable solutions and achieves a significantly higher data rate than other data-driven methods with fixed RIS sensing vectors.

6. REFERENCES

- [1] M. Di Renzo, A. Zappone, M. Debbah, M.-S. Alouini, C. Yuen, J. de Rosny, and S. Tretjakov, "Smart radio environments empowered by reconfigurable intelligent surfaces: How it works, state of research, and the road ahead," *IEEE J. Sel. Areas Commun.*, vol. 38, no. 11, pp. 2450–2525, Jul. 2020.
- [2] R. Liu, M. Li, H. Luo, Q. Liu, and A. L. Swindlehurst, "Integrated sensing and communication with reconfigurable intelligent surfaces: Opportunities, applications, and future directions," June 2022. [Online]. Available: <https://arxiv.org/abs/2206.08518>
- [3] R. S. P. Sankar, S. P. Chepuri, and Y. C. Eldar, "Beamforming in integrated sensing and communication systems with reconfigurable intelligent surfaces," June 2022. [Online]. Available: <https://arxiv.org/abs/2206.07679>
- [4] L. Wei, C. Huang, G. C. Alexandropoulos, C. Yuen, Z. Zhang, and M. Debbah, "Channel estimation for RIS-empowered multi-user MISO wireless communications," *IEEE Trans. Wireless Commun.*, vol. 69, no. 6, pp. 4144–4157, Jun. 2021.
- [5] T. Jiang, H. V. Cheng, and W. Yu, "Learning to reflect and to beamform for intelligent reflecting surface with implicit channel estimation," *IEEE J. Sel. Areas Commun.*, vol. 39, no. 7, pp. 1931–1945, Jul. 2021.
- [6] F. Sohrabi, T. Jiang, W. Cui, and W. Yu, "Active sensing for communications by learning," *IEEE J. Sel. Areas Commun.*, vol. 40, no. 6, pp. 1780–1794, Jun. 2022.
- [7] S. E. Zegrar, L. Afeef, and H. Arslan, "A general framework for ris-aided mmwave communication networks: Channel estimation and mobile user tracking," Sept. 2020. [Online]. Available: <https://arxiv.org/abs/2009.01180>
- [8] Y. Wei, M.-M. Zhao, A. Liu, and M.-J. Zhao, "Channel tracking and prediction for IRS-aided wireless communications," *IEEE Trans. Wireless Commun.*, vol. 22, no. 1, pp. 563–579, 2023.
- [9] J. Yuan, G. C. Alexandropoulos, E. Kofidis, T. L. Jensen, and E. De Carvalho, "Channel tracking for RIS-enabled multi-user SIMO systems in time-varying wireless channels," in *Proc. IEEE Int. Conf. Commun. Workshops (ICC Workshops)*, Jul. 2022, pp. 145–150.
- [10] C. Liu, X. Liu, Z. Wei, S. Hu, D. W. Kwan Ng, and J. Yuan, "Deep learning-empowered predictive beamforming for IRS-assisted multi-user communications," in *Proc. IEEE Global Commun. Conf. (GLOBECOM)*, Madrid, Spain, 2021, pp. 01–07.
- [11] C. Liu, X. Liu, Z. Wei, D. W. K. Ng, and R. Schober, "Scalable predictive beamforming for IRS-assisted multi-user communications: A deep learning approach," Nov. 2022. [Online]. Available: <https://arxiv.org/abs/2211.12644>
- [12] T. L. Jensen and E. De Carvalho, "An optimal channel estimation scheme for intelligent reflecting surfaces based on a minimum variance unbiased estimator," in *Proc. IEEE Int. Conf. Acoust., Speech Signal Process. (ICASSP)*, May 2020, pp. 5000–5004.
- [13] Z. Zhang, T. Jiang, and W. Yu, "Active sensing for localization with reconfigurable intelligent surface," in *Proc. IEEE Int. Conf. Commun. (ICC)*, June 2023, pp. 1–6.
- [14] W. Yu, F. Sohrabi, and T. Jiang, "Role of deep learning in wireless communications," *IEEE BITS Info. Th. Magazine*, pp. 1–14, 2022.
- [15] S. Hochreiter and J. Schmidhuber, "Long short-term memory," *Neural Comput.*, vol. 9, no. 8, pp. 1735–1780, Nov. 1997.
- [16] S. Hochreiter, "The vanishing gradient problem during learning recurrent neural nets and problem solutions," *Int. J. Uncertainty, Fuzziness Knowl.-Based Syst.*, vol. 6, no. 02, pp. 107–116, 1998.
- [17] 3GPP TR 36.814, "Evolved universal terrestrial radio access (E-UTRA); further advancements for E-UTRA physical layer aspects," 3GPP, Technical Report (TR), Mar. 2017, version 9.2.0 (Rel. 9).
- [18] V. Va, H. Vikalo, and R. W. Heath, "Beam tracking for mobile millimeter wave communication systems," in *Proc. IEEE Glob. Conf. Signal Inf. Process. (GlobalSIP)*, 2016, pp. 743–747.
- [19] M. Abadi *et al.*, "Tensorflow: Large-scale machine learning on heterogeneous distributed systems," Mar. 2016. [Online]. Available: <https://arxiv.org/abs/1603.04467>
- [20] D. P. Kingma and J. Ba, "Adam: A method for stochastic optimization," Dec. 2014. [Online]. Available: <https://arxiv.org/abs/1412.6980>